Acta Crystallographica Section B
Structural Science
ISSN 0108-7681

On the polyhedral volume ratios V_A/V_B in perovskites ABX_3

Maxim Avdeev,[a]* El'ad N. Caspi[b] and Sergey Yakovlev[a]

[a]Bragg Institute, ANSTO, Lucas Heights, Australia, and [b]Nuclear Research Center Negev, Department of Physics, Beer Sheva, Israel

Correspondence e-mail: maxim.avdeev@ansto.gov.au

Received 31 October 2006
Accepted 10 January 2007

This paper presents analytical expressions for the calculation of ratios of cation coordination polyhedra volumes (V_A/V_B) for perovskites ABX_3 of the Stokes–Howard diagram directly from atomic coordinates. We show the advantages of quantifying perovskite structure distortion with polyhedral volume ratios rather than with tilting angles, and discuss why space groups with multiple crystallographically inequivalent A or B sites ($I4/mmm$, $Immm$, $P4_2/nmc$ *etc.*) are much less common than those with a single A and B site ($I4/mcm$, $R\bar{3}c$, *Pnma etc.*). Analysis of crystallographic data for approximately 1300 perovskite structures of oxides, halides and chalcogenides from the Inorganic Crystal Structure Database revealed that the most highly distorted perovskites belong to the space group *Pnma* and formally lower-symmetry perovskites ($I2/m$, $I2/a$) are less distorted geometrically. Critical values of the V_A/V_B ratios for the most common phase transitions *Pnma* $\leftrightarrow$ $I4/mcm$ and *Pnma* $\leftrightarrow$ $R\bar{3}c$ are estimated to be ~ 4.85 with the possible intermediate space group *Imma* stable in the very narrow range of $V_A/V_B \simeq 4.8$–4.9. Transitions to post-perovskite $CaIrO_3$-type structures may be expected for $V_A/V_B < 3.8$.

1. Introduction

Perovskites are probably the most studied inorganic materials owing to a variety of interesting physical properties that they possess. According to the Web of Science search engine (ISI, 2006), since the early 1990s on average about 1200 papers on the crystal and magnetic structure and properties of perovskites are published each year by physicists, chemists, geochemists, metallurgists, crystallographers and engineers.

With so much data accumulated throughout the years it is intriguing to look for general trends in the crystallography and crystal chemistry of perovskites. The Inorganic Crystal Structure Database (ICSD; Belsky *et al.*, 2002), containing a few thousand entries for perovskite-type compositions, is the best source of data for such an analysis.

The crucial first step was to identify a universal parameter that would allow perovskites with different space groups to be compared in a way that does not depend on the absolute values of the unit-cell parameters. The following reasoning led us to choose the polyhedral volume ratio (PVR) V_A/V_B, first proposed by Thomas (Thomas & Beitollahi, 1994; Thomas, 1996, 1998), as a parameter which best suits our goals.

1.1. Symmetry considerations: necessary but insufficient

Group-theoretical analysis of phase transitions was first applied to the perovskite structure type decades ago (Barnighausen, 1975; Aleksandrov, 1976), but has been widely recognized only after the recent work of Howard & Stokes

(1998) summarized in Fig. 1. Application of this powerful tool resulted in the revision of crystal structure evolution in a number of perovskites and it will definitely help experimentalists in correct space-group assignments in future. However, as Cotton remarks in his book 'Chemical Application of Group Theory': "...symmetry considerations alone can give us a complete and rigorous answer to the question 'What is possible and what is completely impossible?'. Symmetry considerations alone cannot, however, tell us how likely it is that the possible things will actually take place" (Cotton, 1990, p. 4). Obviously, for practical purposes a bridge from the symmetry approach to structural characteristics is needed and for perovskites such a connection can be established *via* the geometric consideration of deviations from the ideal arrangement of ideal octahedra and cuboctahedra of the cubic aristotype. At present, these are frequently discussed in terms of tilting angles.

1.2. Tilting angles: Convenience at the price of generality

The tilting angles of BX_6 octahedra are widely used for both the classification of distorted perovskites (Glazer, 1972, 1975) and as a quantitative measure of perovskite structure distortion. The latter was first applied to rhombohedrally distorted perovskites (Michel *et al.*, 1971; Megaw, 1973) and then was extended to tetragonal and orthorhombic perovskites (Mitchell, 2002). Indeed, tilting angles are convenient for intercomparison of perovskites *within the same tilt system* or as order parameters for phase transitions, as zeroing of one or more tilting angles corresponds to the phase transition to a higher symmetry. However, we saw the following obstacles to using tilting angles as a universal parameter easily applicable to all known distorted perovskites ABX_3:

The geometry of distorted perovskites ABX_3 was explored chronologically before and/or without connection with group-theoretical analysis of phase transitions in perovskites; no attempt to develop a unified approach to using tilting angles across different tilting systems has been made. Tetragonal, rhombohedral and orthorhombic perovskite structures are traditionally discussed in the literature in terms of the rotation of BX_6 octahedra around different directions of the aristotype cubic cell, *i.e.* $[001]_p$, $[111]_p$, and a combination of $[001]_p$ and $[110]_p$, respectively. This approach complicates the presentation of phase transitions such as $R\bar{3}c \leftrightarrow Pnma$, $R\bar{3}c \leftrightarrow Imma$ *etc.* In Fig. 2 we illustrate how mixing different types of tilting angles in phase diagrams may give the misleading impression that some drastic changes occur with the structure during the phase transition, while in fact distortion increases gradually.

To the best of our knowledge simple formulae for estimating tilting angles using cell parameters or atomic coordinates were reported for only about half of the space groups of the Howard–Stokes diagram, *i.e.* for tetragonal, orthorhombic and rhombohedral ones (Mitchell, 2002). For space groups of lower symmetry the definition of the tilting angle itself is less clear as octahedra may be significantly deformed. For example, in monoclinic $Ca(Sb_{0.2}Mn_{0.8})O_3$ perovskite (space group $P2_1/m$, ICSD #99429; Poltavets *et al.*, 2004), the O_{apical}—(Sb,Mn)—$O_{equatorial}$ angle is $\sim 80.3^\circ$. In order to use the angle of rotation of such an octahedron around some crystallographic directions one would first need to clarify whether the rotation of the M—O_{apical} bond or of the equatorial plane of the octahedron is considered, or some averaging scheme would have to be used.

1.3. Polyhedral volume ratios

Both tilting angles around any axis and deformation of A- and B-site polyhedra may be convoluted to a single parameter, *i.e.* the ratio of cation coordination polyhedra volumes V_A/V_B that was proposed for the quantitative description of perovskite structures by Thomas (Thomas & Beitollahi, 1994;

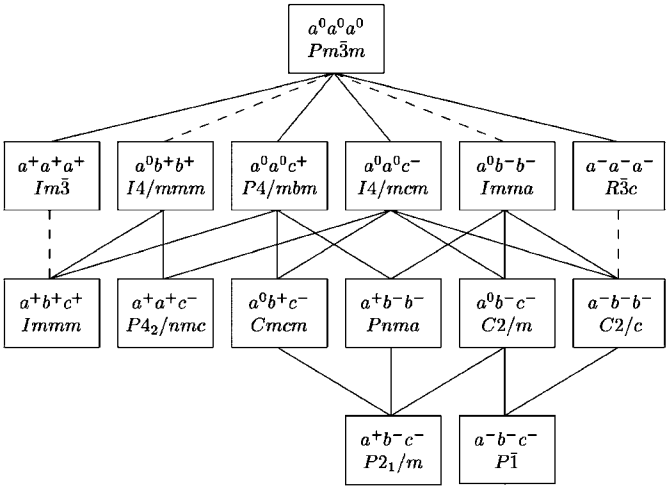

Figure 1
Howard–Stokes diagram for disordered ABX_3 perovskites (reproduced from Howard & Stokes, 2002). Solid and dashed lines indicate phase transitions of second and first order, respectively.

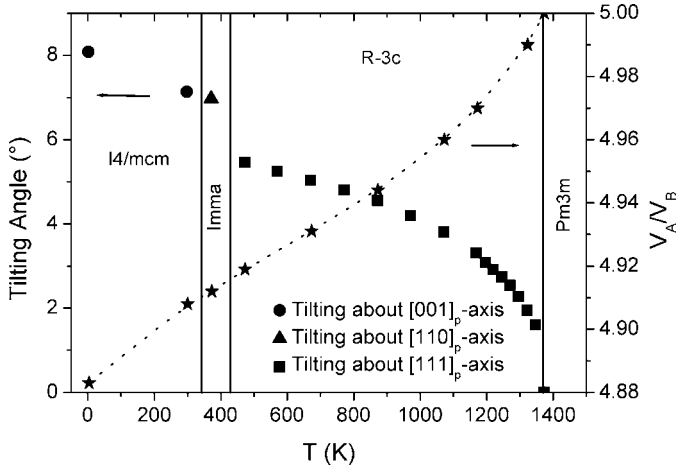

Figure 2
Tilting angles (circles, triangles and squares) from Fu & Ijdo (2006) and polyhedral volume ratios (stars) calculated using formulae from Table 1 as a function of temperature for $CeAlO_3$.

Table 1
Polyhedral volume ratios for ABX_3 perovskites in terms of atomic coordinates.

Glazer tilt system	Space group (Wyckoff sequence)	Unit cell	Atomic positions	Polyhedral volume ratios
$a^0a^0a^0$	#2 *Pm*3*m* (dba)	$a = b = c \equiv a_p$	*A*: 1(*b*) $\frac{1}{2},\frac{1}{2},\frac{1}{2}$ *B*: 1(*a*) 0,0,0 *X*: 3(*d*) $\frac{1}{2}$,0,0	$\frac{V_A}{V_B} = 5$
$a^0a^0c^-$	#140 *I*4/*mcm* (hcba)	$a = b \simeq 2^{1/2}a_p$ $c \simeq 2a_p$	*A*: 4(*b*) 0,$\frac{1}{2},\frac{1}{4}$ *B*: 4(*c*) 0,0,0 *X*1: 4(*a*) 0,0,$\frac{1}{4}$ *X*2: 8(*h*) $x, x+\frac{1}{2}$, 0; $x \simeq \frac{1}{4}$	$\frac{V_A}{V_B} = \frac{3}{1-4x(X2)+8x(X2)^2} - 1$
$a^0a^0c^+$	#127 *P*4/*mbm* (gcba)	$a = b \simeq 2^{1/2}a_p$ $c \simeq a_p$	*A*: 2(*c*) 0,$\frac{1}{2},\frac{1}{2}$ *B*: 2(*a*) 0,0,0 *X*1: 2(*b*) 0,0,$\frac{1}{2}$ *X*2: 4(*g*) $x, x+\frac{1}{2}$,0; $x \simeq \frac{1}{4}$	$\frac{V_A}{V_B} = \frac{3}{1-4x(X2)+8x(X2)^2} - 1$
$a^0b^-b^-$	#74 *Imma* (ge2a)	$a \simeq c \simeq 2^{1/2}a_p$ $b \simeq 2a_p$	*A*: 4(*e*) 0, $\frac{1}{4}$, *z*; $z \simeq \frac{1}{2}$ *B*: 4(*a*) 0,0,0 *X*1: 4(*e*) 0, $\frac{1}{4}$, *z*; $z \simeq 0$ *X*2: 8(*g*): $\frac{1}{4}$, *y*, $\frac{1}{4}$; $y \simeq 0$	$\frac{V_A}{V_B} = \frac{6}{1-16y(X2)z(X1)} - 1$
	(ge2b)	$a \simeq c \simeq 2^{1/2}a_p$ $b \simeq 2a_p$	*A*: 4(*e*) 0, $\frac{1}{4}$, *z*; $z \simeq 0$ *B*: 4(*b*) 0,0,$\frac{1}{2}$ *X*1: 4(*e*) 0, $\frac{1}{4}$, *z*; $z \simeq \frac{1}{2}$ *X*2: 8(*g*): $\frac{1}{4}$, *y*, $\frac{3}{4}$; $y \simeq 0$	$\frac{V_A}{V_B} = \frac{6}{1+8y(X2)(1-2z(X1))} - 1$
$a^0b^-c^-$	#12 *I*2/*m* (i2hge)	$a \simeq c \simeq 2^{1/2}a_p$ $b \simeq 2a_p$ $\beta \simeq 90^\circ$	*A*: 4(*i*) *x*, 0, *z*; $x \simeq \frac{1}{4}$, $z \simeq \frac{3}{4}$ *B*: 4(*e*) $\frac{1}{4}, \frac{1}{4}, \frac{1}{4}$ *X*1: 4(*i*) *x*, 0, *z*; $x \simeq z \simeq \frac{1}{4}$ *X*2: 4(*g*) 0, *y*, 0; $y \simeq \frac{1}{4}$ *X*3: 4(*h*) $\frac{1}{2}$, *y*, 0; $y \simeq \frac{1}{4}$	$\frac{V_A}{V_B} = \frac{3}{2\lvert 2z(X1)(y(X2)-y(X3))+2x(X1)(y(X2)+y(X3))-y(X2)-x(X1)\rvert} - 1$
$a^0b^+c^-$	#63 *Cmcm* (gfedc2)	$a \simeq b \simeq c \simeq 2a_p$	A1: 4(*c*) 0, *y*, $\frac{1}{4}$; $y \simeq 0$ *A*2: 4(*c*) 0, *y*, $\frac{1}{4}$; $y \simeq \frac{1}{2}$ *B*: 8(*d*) $\frac{1}{4}, \frac{1}{4}, 0$	$\frac{V_{A_1}}{V_B} = 2\frac{\begin{pmatrix}2z(X2)(y(X2)(1-4x(X3))+x(X1)(1-4y(X3)))\\+y(X2)+2x(X1)y(X2)+x(X1)\end{pmatrix}}{\begin{pmatrix}(1-4x(X1))(y(X2)-4z(X2)y(X3))\\+x(X1)-4x(X1)z(X2)+4z(X2)x(X3)\end{pmatrix}}$ $\frac{V_{A_2}}{V_B} = -\frac{\begin{pmatrix}4z(X2)(x(X1)(1-4y(X3))-y(X2)(1-4x(X3))+2(y(X3)-x(X3)))\\+4(x(X1)y(X2)-x(X1)-y(X2))+3\end{pmatrix}}{x(X1)+4z(X2)(x(X3)-x(X1))+(1-4x(X1))(y(X2)-4z(X2)y(X3))}$ $\langle V_A\rangle/V_B = \frac{3}{2\begin{pmatrix}x(X1)+4z(X2)(x(X3)-x(X1))\\+(1-4x(X1))(y(X2)-4z(X2)y(X3))\end{pmatrix}} - 1$

Table 1 (continued)

Glazer tilt system	Space group (Wyckoff sequence)	Unit cell	Atomic positions	Polyhedral volume ratios
			*X*1: 8(*e*) $x, 0, 0$; $x \simeq \frac{1}{4}$	
			*X*2: 8(*f*) $0, y, z$; $y \simeq \frac{1}{4}$, $z \simeq 0$	
			*X*3: 8(*g*) $x, y, \frac{1}{4}$; $x \simeq y \simeq \frac{1}{4}$	
$a^0b^+b^+$	#139 *I*4/*mmm* (nhfcba)	$a = b \simeq c \simeq 2a_p$	*A*1: 2(*a*) 0,0,0	$\frac{V_{A_1}}{V_B} = \frac{4z(X2)(y(X2)+4x(X1))}{2x(X1)+2z(X2)-y(X2)-8x(X1)z(X2)}$
			*A*2: 2(*b*) $0, 0, \frac{1}{2}$	$\frac{V_{A_2}}{V_B} = \frac{4(x(X1)+z(X2)+y(X2)z(X2)-1)}{8x(X1)z(X2)-2x(X1)+y(X2)-2z(X2)} - 2$
			*A*3: 4(*c*) $\frac{1}{2}, 0, 0$	$\frac{V_{A_3}}{V_B} = \frac{3-8y(X2)+4y(X2)^2}{4y(X2)(2x(X1)+2z(X2)-y(X2)-8x(X1)z(X2))}$
			B: 8(*f*) $\frac{1}{4}, \frac{1}{4}, \frac{1}{4}$	$\langle V_A \rangle / V_B = \frac{3}{8y(X2)(2x(X1)+2z(X2)-y(X2)-8x(X1)z(X2))} - 1$
			*X*1: 8(*h*) $x, x, 0$; $x \simeq \frac{1}{4}$	
			*X*2: 16(*n*) $0, y, z$; $y \simeq z \simeq \frac{1}{4}$	
$a^-a^-a^-$	#167 $R\bar{3}c$ (eba)	$a = b \simeq 2^{1/2}a_p$ $c \simeq 2(3)^{1/2}a_p$	*A*: 6(*a*) $0, 0, \frac{1}{4}$	$\frac{V_A}{V_B} = \frac{3}{2\left(1-3x(X1)+3x(X1)^2\right)} - 1$
			B: 6(*b*) $0, 0, 0$	
			O: 18(*e*) $x, 0, \frac{1}{4}$; $x \simeq \frac{1}{2}$	
$a^-b^-b^-$	#15 *I*12/*a*1 (fe2b)	$a \simeq 2a_p$	*A*: 4(*e*) $\frac{1}{4}, y, 0$; $y \simeq 0$	$\frac{V_A}{V_B} = \frac{3}{\left(\begin{array}{l}6z(X2)-4y(X1)-4x(X2)+2y(X2)\\+8y(X1)x(X2)-8z(X2)y(X2)+1\end{array}\right)} - 1$
		$b \simeq c \simeq 2^{1/2}a_p$	*B*: 4(*b*) $0, \frac{1}{2}, 0$	
			*X*1: 4(*e*) $\frac{1}{4}, y, 0$; $y \simeq \frac{1}{2}$	
			*X*2: 8(*f*) x, y, z; $x \simeq \frac{1}{2}$, $y \simeq \frac{3}{4}$, $z \simeq \frac{1}{4}$	
$a^+b^-b^-$	#62 *Pnma* (dc2a)	$a \simeq c \simeq 2^{1/2}a_p$	*A*: 4(*c*) $x, 1/4, z$; $x \simeq \frac{1}{2}$, $z \simeq 0$	$\frac{V_A}{V_B} = \frac{3}{2((1-4z(X2))(x(X2)-4x(X1)y(X2))-4y(X2)z(X1)+z(X2))} - 1$
$a^+a^-a^-$		$b \simeq 2a_p$	*B*: 4(*a*) $0, 0, 0$	
			*X*1: 4(*c*) $x, \frac{1}{4}, z$; $x \simeq z \simeq 0$	
			*X*2: 8(*d*) x, y, z; $x \simeq z \simeq \frac{1}{4}$, $y \simeq 0$	
	Pnma (dc2b)	$a \simeq c \simeq 2^{1/2}a_p$	*A*: 4(*c*) $x, \frac{1}{4}, z$; $x \simeq z \simeq \frac{1}{2}$	$\frac{V_A}{V_B} = \frac{3}{2(3-4z(X2))(x(X2)-4x(X1)y(X2))+4y(X2)(1-2z(X1))+2z(X2)-1} - 1$
		$b \simeq 2a_p$	*B*: 4(*a*) $\frac{1}{2}, 0, 0$	
			*X*1: 4(*c*) $x, \frac{1}{4}, z$; $x \simeq 0$, $z \simeq \frac{1}{2}$	

Table 1 (continued)

Glazer tilt system	Space group (Wyckoff sequence)	Unit cell	Atomic positions	Polyhedral volume ratios
			$X2$: 8(d) x, y, z; $x \simeq \frac{1}{4}$, $y \simeq 0$, $z \simeq \frac{3}{4}$	
	Pbnm (dc2a)	$a \simeq b \simeq 2^{1/2}a_p$	A: 4(c) $x, y, \frac{1}{4}$; $x \simeq 0$; $y \simeq \frac{1}{2}$	$\frac{V_A}{V_B} = \frac{3}{2((1-4x(X2))(y(X2)-4y(X1)z(X2))-4x(X1)z(X2)+x(X2))} - 1$
		$c \simeq 2a_p$	B: 4(a) 0, 0, 0	
			$X1$: 4(c) $x, y, \frac{1}{4}$; $x \simeq y \simeq 0$	
			$X2$: 8(d) x, y, z; $x \simeq y \simeq \frac{1}{4}$, $z \simeq 0$	
	Pbnm (dc2b)	$a \simeq b \simeq 2^{1/2}a_p$	A: 4(c) $x, y, \frac{1}{4}$; $x \simeq 0$; $y \simeq \frac{1}{2}$	$\frac{V_A}{V_B} = \frac{3}{2(3-4x(X2))(y(X2)-4y(X1)z(X2))-4z(X2)(4x(X2)-2x(X1)-3)+2x(X2)-1} - 1$
		$c \simeq 2a_p$	B: 4(a) $\frac{1}{2}$, 0, 0	
			$X1$: 4(c) $x, y, \frac{1}{4}$; $x \simeq 0$, $y \simeq \frac{1}{2}$	
			$X2$: 8(d) x, y, z; $x \simeq \frac{3}{4}$, $y \simeq \frac{1}{4}$, $z \simeq 0$	
$a^+b^-c^-$	#11 $P2_1/m$ (f2e4cb)	$a \simeq c \simeq 2^{1/2}a_p$	$A1$: 2(e) $x, \frac{1}{4}, z$; $x \simeq z \simeq 0$	$\frac{\langle V_A\rangle}{\langle V_B\rangle} = \frac{\begin{pmatrix} 2-x(X4)+z(X4)+2x(X3)+4y(X3)(1-2x(X2))+4z(X2)(y(X3)-y(X4)) \\ +4x(X1)(y(X4)-y(X3))+4x(X4)(y(X3)+z(X3))-4z(X4)(x(X3)+y(X3)) \\ +(4y(X4)-1)(z(X3)-x(X3))+8(x(X3)y(X4)-x(X4)y(X3))(z(X1)+z(X2)) \\ +8(y(X3)z(X4)-y(X4)z(X3))(x(X1)+x(X2)) \end{pmatrix}}{\begin{pmatrix} x(X3)(4z(X4)-3)-4z(X3)(y(X4)+x(X4))+4y(X4)z(X2)(1-2x(X3)) \\ -4y(X3)z(X2)(1-2x(X4))+4y(X3)(1-2z(X4))(x(X1)+x(X2))+x(X4) \\ +4(1-2z(X1))(x(X3)y(X4)-x(X4)y(X3))+(1-4y(X3))(1-z(X4)) \\ +8y(X4)z(X3)(x(X1)+x(X2))+z(X3)-4x(X1)y(X4)+4x(X2)y(X3) \end{pmatrix}}$
		$b \simeq 2a_p$	$A2$: 2(e) $x, \frac{1}{4}, z$; $x \simeq z \simeq \frac{1}{2}$	
		$\beta \simeq 90^\circ$	$B1$: 2(b) $\frac{1}{2}$, 0, 0	
			$B2$: 2(c) 0, 0, $\frac{1}{2}$	
			$X1$: 2(e) $x, \frac{1}{4}, z$; $x \simeq 0$, $z \simeq \frac{1}{2}$	
			$X2$: 2(e) $x, \frac{1}{4}, z$; $x \simeq \frac{1}{2}$, $z \simeq 0$	
			$X3$: 4(f) x, y, z; $x \simeq z \simeq \frac{1}{4}$, $y \simeq 0$	
			$X4$: 4(f) x, y, z; $x \simeq \frac{1}{4}$, $y \simeq 0$, $z \simeq \frac{3}{4}$	

Table 1 (continued)

Glazer tilt system	Space group (Wyckoff sequence)	Unit cell	Atomic positions	Polyhedral volume ratios
$a^+a^+c^-$	#137 $P4_2/nmc$ (g2fedba)	$a \simeq c \simeq 2a_p$	$A1$: 2(a) $\frac{3}{4}, \frac{1}{4}, \frac{3}{4}$ $A2$: 2(b) $\frac{3}{4}, \frac{1}{4}, \frac{1}{4}$ $A3$: 2(c) $\frac{1}{4}, \frac{1}{4}, z$; $z \simeq \frac{1}{4}$ B: 8(e) 0, 0, 0 $X1$: 8(g) $\frac{1}{4}, y, z$; $y \simeq z \simeq 0$ $X2$: 8(g) $\frac{1}{4}, y, z$; $y \simeq z \simeq \frac{1}{2}$ $X3$: 8(f) $x, -x, \frac{1}{4}$; $x \simeq \frac{1}{2}$	$\frac{V_{A_1}}{V_B} = \frac{2\begin{pmatrix}2(2y(X1)-1)(1-4x(X3))+4y(X2)(1-3z(X1)-4x(X3))\\+4z(X2)(1+4y(X1))(4x(X3)-y(X2))-z(X2)(1+4y(X1))\\+4(4y(X2)-3)(y(X1)z(X1)+4z(X1)x(X3))+9z(X1)\end{pmatrix}}{\begin{pmatrix}3+16y(X2)y(X1)-2(3-4x(X3))(1+4y(X1))\\-8(1-2x(X3))(z(X1)(3-4y(X2))-z(X2)(1+4y(X1)))\end{pmatrix}}$ $\frac{V_{A_2}}{V_B} = \frac{2\begin{pmatrix}3+24x(X3)(2y(X1)+1)-4(4y(X1)+1)(y(X2)z(X2)+3)\\+(4y(X2)-3)(13z(X1)+4)+4z(X1)(4y(X2)-3)(y(X1)-4x(X3))\\+z(X2)(1+4y(X1))(15-16x(X3))+16y(X2)(y(X1)-x(X3))\end{pmatrix}}{\begin{pmatrix}3+8y(X1)(3-2y(X2))-8x(X3)(1+4y(X1))\\+8(2x(X3)-1)(z(X2)(1+4y(X1))+z(X1)(4y(X2)-3))\end{pmatrix}}$ $\frac{V_{A_3}}{V_B} = \frac{1-12y(X2)+4y(X1)+16y(X2)y(X1)}{\begin{pmatrix}8(2x(X3)-1)(4y(X2)z(X1)+4y(X1)z(X2)-3z(X1)+z(X2))\\+2(4y(X1)+1)(3-4x(X3))-16y(X2)y(X1)-3\end{pmatrix}}$ $\frac{\langle V_A\rangle}{V_B} = \frac{6}{\begin{pmatrix}16y(X2)y(X1)-2(4y(X1)+1)(3-4x(X3))-8(z(X2)-3z(X1))(2x(X3)-1)\\-32(y(X1)z(X2)+y(X2)z(X1))(2x(X3)-1)+3\end{pmatrix}}-1$
$a^+a^+a^+$	#204 $Im\bar{3}$ (gcba)	$a=b=c \simeq 2a_p$	$A1$: 2(a) 0, 0, 0 $A2$: 6(b) $0, \frac{1}{2}, \frac{1}{2}$ B: 8(c) $\frac{1}{4}, \frac{1}{4}, \frac{1}{4}$ $X1$: 24(g) 0, y, z; $y \simeq z \simeq \frac{1}{4}$	$\frac{V_{A_1}}{V_B} = \frac{4\left(z(X1)^3+y(X1)^3+3z(X1)^2y(X1)\right)}{3y(X1)^2+3z(X1)^2-4y(X1)^3-4z(X1)^3-3z(X1)y(X1)}$ $\frac{V_{A_2}}{V_B} = \frac{8y(X1)^3+8z(X1)^3+24z(X1)^2y(X1)-3}{6\left(4y(X1)^3+4z(X1)^3-3y(X1)^2-3z(X1)^2+3y(X1)z(X1)\right)}-\frac{4}{3}$ $\frac{\langle V_A\rangle}{V_B} = \frac{3}{8\left(3y(X1)^2+3z(X1)^2-4y(X1)^3-4z(X1)^3-3z(X1)y(X1)\right)}-1$
$a^+b^+c^+$	#71 $Immm$, (nmlkdcba)	$a \simeq b \simeq c \simeq 2a_p$	$A1$: 2(a) 0, 0, 0 $A2$: 2(b) $0, \frac{1}{2}, \frac{1}{2}$ $A3$: 2(c) $\frac{1}{2}, \frac{1}{2}, 0$ $A4$: 2(d) $\frac{1}{2}, 0, \frac{1}{2}$ B: 8(k) $\frac{1}{4}, \frac{1}{4}, \frac{1}{4}$ $X1$: 8(l) 0, y, z; $y \simeq z \simeq \frac{1}{4}$ $X2$: 8(m) x, 0, z; $x \simeq z \simeq \frac{1}{4}$ $X3$: 8(n) x, y, 0; $x \simeq y \simeq \frac{1}{4}$	$\frac{V_{A_1}}{V_B} = 2\frac{(z(X1)+z(X2))(2x(X3)y(X1)+x(X2)(2y(X3)+y(X1)))}{\begin{pmatrix}z(X1)y(X3)+z(X2)(y(X1)-y(X3))+x(X2)y(X3)(1-4z(X1))\\+x(X3)z(X2)(1-4y(X1))+(y(X1)-z(X1))(x(X3)-x(X2))\end{pmatrix}}$ $\frac{V_{A_2}}{V_B} = \frac{\begin{pmatrix}(z(X2)-z(X1))(8(y(X1)(x(X2)+2x(X3))+y(X3)(1-2x(X2))-x(X3))-4x(X2)+6(1-2y(X1)))\\+(1-2y(X1))(3-4x(X3))-2x(X2)+4y(X3)-8x(X2)y(X3)+4x(X2)y(X1)\end{pmatrix}}{4\begin{pmatrix}z(X1)y(X3)+z(X2)(y(X1)-y(X3))+x(X2)y(X3)(1-4z(X1))\\+x(X3)z(X2)(1-4y(X1))+(y(X1)-z(X1))(x(X3)-x(X2))\end{pmatrix}}$ $\frac{V_{A_3}}{V_B} = 2\frac{\begin{pmatrix}(z(X1)+z(X2))(y(X1)(2x(X3)-x(X2)-1)+x(X2)(2y(X3)-1))\\+x(X2)y(X1)-2x(X2)y(X3)+x(X2)+y(X1)-2x(X3)y(X1)\end{pmatrix}}{\begin{pmatrix}z(X1)y(X3)+z(X2)(y(X1)-y(X3))+x(X2)y(X3)(1-4z(X1))\\+x(X3)z(X2)(1-4y(X1))+(y(X1)-z(X1))(x(X3)-x(X2))\end{pmatrix}}$ $\frac{V_{A_4}}{V_B} = \frac{\begin{pmatrix}2(z(X2)-z(X1))(4x(X3)(2y(X1)-1)+(2x(X2)-1)((3-2y(X1))-4y(X3)))\\+(3-4y(X3))(1-2x(X2))-8x(X3)y(X1)+4x(X2)y(X1)-2y(X1)+4x(X3)\end{pmatrix}}{4\begin{pmatrix}z(X1)y(X3)+z(X2)(y(X1)-y(X3))+x(X2)y(X3)(1-4z(X1))\\+x(X3)z(X2)(1-4y(X1))+(y(X1)-z(X1))(x(X3)-x(X2))\end{pmatrix}}$ $\frac{\langle V_A\rangle}{V_B} = \frac{3}{8\begin{pmatrix}z(X1)y(X3)+z(X2)(y(X1)-y(X3))+x(X2)y(X3)(1-4z(X1))\\+x(X3)z(X2)(1-4y(X1))+(y(X1)-z(X1))(x(X3)-x(X2))\end{pmatrix}}-1$

Thomas, 1998). The approach is well suited for the perovskite structure type as the three-dimensional space of its crystal structure can be partitioned into A- and B-site cation polyhedra without voids, so the equation

$$V = \sum_{i=1}^{Z} V_{A_i} + \sum_{j=1}^{Z} V_{Bj} \qquad (1)$$

will always be valid (where V is the volume of the unit cell, V_A and V_B are the volumes of A- and B-site cation polyhedra, and Z is the number of formula units ABX_3 in the unit cell).

Using an empirical analysis of the experimental data Thomas demonstrated that V_A/V_B ratios are related to tilting angles and since formulae for tilting angles were developed in parallel, the polyhedral volume ratios (PVR) method could also be easily applied to the same perovskite modifications. The method has been shown to be quite accurate for the prediction of phase transitions in orthorhombic (Thomas,

1998; Magyari-Ḱope *et al.*, 2001, 2002*a*,*b*) and rhombohedral (Thomas, 1996; Zhao *et al.*, 2004) perovskites, but even after that the approach has not been widely adopted as 'no general recipe for the determination of the independent variables, V and V_A/V_B, is provided' (Magyari-Köpe *et al.*, 2002*a*).

Alternatively, V_A/V_B ratios can be calculated numerically using, for example, the popular program *IVTON* (Balic Zunic & Vickovic, 1996). However, owing to significant variation in the degree of distortion of perovskites, great care is needed when adjusting the limits for searching the coordinating atoms, which makes it difficult to process the ICSD data in an automatic mode. In addition, we provide the evidence that numerical calculations according to the algorithms designed to construct only convex polyhedra not only do not always hold (1) true, but in some cases even lead to qualitatively misleading results when applied to perovskites.

1.4. Perovskites under non-ambient conditions

Today the relative stability of the different modifications of the perovskite structure type can be estimated with a wide range of methods, from simple geometric considerations based on the concept of ionic radii (Goldschmidt, 1926) and bond-valence approach (Brown & Altermatt, 1985), as implemented, for example, in the *SPUDS* software (Lufaso & Woodward, 2001), to first-principles calculations. However, most of these methods rely on tabulated values of radii, bond-valence parameters, interatomic potentials *etc.*, which are well established for room temperature but are often unknown for non-ambient conditions (high pressure, low/high temperature *etc.*). First-principle studies are also too non-trivial and time consuming to be used in routine structural studies.

It was already proposed that the relative compressibilities of *A*- and *B*-site polyhedra determine whether a perovskite structure will become more or less distorted under high pressure (Andrault & Poirier, 1991), but the number of analysed structures was too small to draw quantitative conclusions.

The above-mentioned considerations motivated us to explore and modify the PVR method. Notice that we do not use the term global parameterization method (GPM) as introduced by Thomas (Thomas, 1998), because we take a different approach and instead of relating V_A/V_B ratios to tilting angles, we express ratios directly in terms of atomic coordinates. We overcame the shortcomings of the original approach, *i.e.*

(i) we do not employ any empirical coefficients and present the exact expressions of calculation of PVRs, and

(ii) PVRs are calculated directly from atomic coordinates and therefore no intermediate calculations of distances or angles are required.

Since PVRs are calculated directly from experimental structural data under any conditions and do not depend on any tabulated parameters, they can be used for a unified description of crystal structure evolution as a function of chemical composition, temperature, pressure *etc.* Finally, we estimate the critical values at which phase transitions will occur in such parametric studies.

2. Analysis details and conventions

The formulae of the V_A/V_B ratios in ABX_3 disordered perovskites in terms of atomic coordinates were derived using linear algebra in combination with group–subgroup relations and are presented in Table 1. While in general we followed the unit-cell descriptions and space-group settings given by Woodward in Table 5 (Woodward, 1997), for several space groups we present more than one set of formulae. For example, we found that crystal structures with the space group *Imma* are more often published with the (ge2b) Wyckoff sequence rather than with (ge2a) as used by Woodward, so we present formulae for both. Similarly, in addition to the *Pnma* space group with Wyckoff sequence (dc2b), we also considered three other widely used settings: *Pnma* (dc2a), *Pbnm* (dc2a) and *Pbnm* (dc2b). Other settings such as *Pcmn*, *Pmcn*, *Pmnb etc.* were not considered as altogether they cover less than 3% of the total number of ABX_3 perovskites with space group 62 present in the ICSD.

For all the space groups we assumed *A*- and *B*-site polyhedra to have 12 and 6 vertices, respectively, in order to preserve the condition (1). We are conscious that an unambiguous definition of coordination number is one of the fundamental problems of inorganic solid-state chemistry and many would argue that in the case of highly distorted perovskites the coordination number of the *A* site is 10, 9, 8 or even 4 + 2. However, in order to place all perovskites on the same scale and in our effort to devise a universal reference for this family of compounds, it is essential to consider the geometry of the crystal structure from the same viewpoint. As shown in the following text, the self-consistency of the results supports our approach.

For space groups with multiple *A* sites we present the formulae both for PVRs of individual *i*th polyhedra V_{Ai}/V_B and for the average *A*-site volume $\langle V_A\rangle/V_B$. We present the formula for the ratio of the average polyhedral volumes $\langle V_A\rangle/\langle V_B\rangle$ only for the space group $P2_1/m$ having two *A* sites and two *B* sites as it is arguable how the volumes of individual *B*-site polyhedra should be handled in the denominators of PVRs.

3. Results and discussion

3.1. PVR distribution statistics

The statistics of PVR distribution are presented in Fig. 3, revealing the following features:

(i) Most space groups are characterized by PVR distribution with well defined maxima positions and boundaries that allowed us to estimate the critical values of PVRs at which the perovskite structure undergoes a phase transition from one space group to another. We estimate the critical values of PVRs for the most common transitions *Pnma* $\leftrightarrow$ *I*4/*mcm* and *Pnma* $\leftrightarrow$ $R\bar{3}c$ to be ~ 4.85 with the possible intermediate

space group *Imma* which is stable in the very narrow range of $V_A/V_B \simeq 4.8$–4.9.

(ii) The most highly distorted perovskites belong to the space group *Pnma* reaching PVRs as low as 3.8, much lower than any known monoclinic simple perovskites ABX_3. This is in agreement with the fact that the pressure-induced transition of a perovskite-type structure to the so-called 'post-perovskite' $CaIrO_3$-type modification occurs directly from *Pnma* without any intermediate perovskite phases of lower symmetry (Murakami *et al.*, 2004).

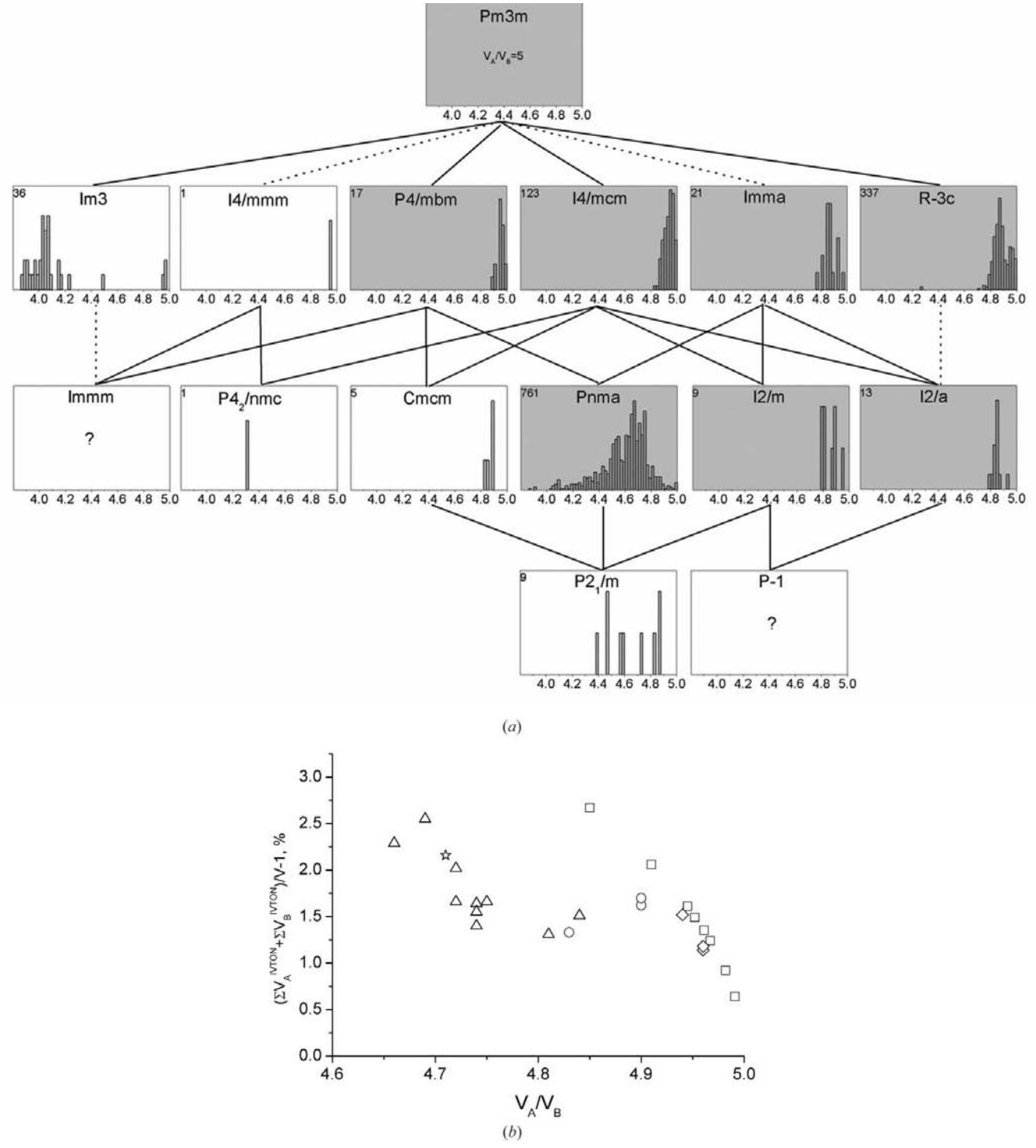

Figure 3
Top: Distribution of PVRs for ABX_3 perovskites. The number in the upper-left corner of each pane indicates the total number of structures in the histogram. The binning interval is 0.02. The shading indicates structures with a single *A* and *B* site (see §3.3 for discussion). Bottom: Deviation of the sum of all polyhedra volumes calculated with *IVTON* from the total unit-cell volume as a function PVR. Squares, circles, triangles, diamonds and stars indicate examples of structures with *P*4/*mbm*, *Cmcm*, *Pnma*, *Im*3 and $P2_1/m$ space groups, respectively.

(iii) The number of ABX_3 perovskite structures with a single A and B site present in the ICSD (shaded panes in Fig. 3) is significantly higher than that of structures with multiple A or B sites. This observation, as well as the origin of an anomalously high number of perovskites having the space group $Im3$ with low PVRs of $\sim$ 3.85–4.2, are discussed in §3.3.

The structural data used in the analysis were not checked for reliability using, for example, R factors. Fig. 3 may therefore include ICSD entries with incorrectly assigned space groups. However, we believe that the number of analysed structures is large enough for statistics of PVR distribution not to be significantly affected by those rare instances.

3.2. Exact expressions *versus* numerical calculations

Since in the cubic perovskite structure ideal cuboctahedra coordinating A sites share square faces, any deformation resulting in their non-planarity will split the faces to triangles. After that only one of two cuboctahedra that shared an originally square face can stay convex and another will become concave. Unfortunately, most of the computer programs currently used for the calculation of polyhedral volumes in crystal structures, including *IVTON* (Balic Zunic & Vickovic, 1996), in such a situation will treat both cuboctahedra as convex, counting the same space twice. As a result, the condition (1) will no longer hold true and V_A/V_B ratios will be overestimated. When comparing the results of our calculations using the formulae from Table 1 with those performed using *IVTON* we encountered deviations of the sum of all polyhedra volumes from the total unit-cell volume V up to 4%. In some cases such deviations result even in a qualitatively different picture. For example, for the $CsDyBr_3$ structure (ICSD #300285, space group $P4/mbm$, $Z = 2$) according to *IVTON* $V_A^{IVTON} = 164.68$ Å^3 and $V_B^{IVTON} = 32.73$ Å^3, which results in $Z(V_A^{IVTON} + V_B^{IVTON}) = 394.82$ Å^3, while the cell volume is 386.85 Å^3. Moreover, while the correct V_A/V_B equals 4.91, the values obtained with *IVTON* produce a misleading result $V_A^{IVTON}/V_B^{IVTON} = 5.03$ that is higher than that for the undistorted cubic perovskite and is typical for 'hexagonal perovskites' with face-sharing octahedra.

This kind of problem does not affect the space groups $I4/mcm$, $Imma$, $R\bar{3}c$, $I2/m$ and $I2/a$, in which the planarity of the square faces of the cuboctahedra is preserved during distortion. For all other space groups, the difference between the sum of all the polyhedra calculated with *IVTON* and the total unit-cell volume generally increases with increasing structure distortion, as illustrated in Fig. 3.

3.3. 'Disordered by symmetry' *versus* 'multiple cation site' perovskites

As can be seen in Fig. 3 the number of structures with a single A and B site is significantly higher than that of structures with multiple crystallographically inequivalent A and/or B sites. The analysis of the geometry of perovskites provides the explanation.

As follows from the formulae in Table 1 for structures with multiple cation positions (non-shaded panes in Fig. 3), polyhedral volumes for individual A-site cations have a different dependence on atomic coordinates. We illustrate this using the example of the space group $Im3$ which has only two atomic coordinate variables, $y(X1)$ and $z(X1)$, so the effect can be easily visualized. The polyhedral volumes normalized by unit-cell volume for two crystallographically inequivalent A sites, $2a$(0,0,0) and $6b$(0,1/2,1/2), as functions of $y(X1)$ and $z(X1)$, are presented in Fig. 4(a). The volumes $VA(2a)$ and $VA(6b)$ will be equal only for certain combinations of $y(X1)$ and $z(X1)$, presented in Fig. 4 by a solid line. For all other combinations of $y(X1)$ and $z(X1)$ $VA(2a)$ will be either smaller or larger than $VA(6b)$ (Fig. 4b). That makes phase transitions to this structure thus having, in general, energetically different coordinations of $A(2a)$ and $A(6b)$, to be unfavourable for *simple* ABX_3 *compounds* and additional factors are required to stabilize the structure. Experimental points in Fig. 4 (bottom) correspond to the well known family of $Ca_3CuTi_4O_{12}$ type which is stabilized by the simultaneous presence of the Ca^{2+} cation in the larger ($2a$) site and of Cu^{2+} in the much smaller ($6b$) site which is highly distorted by the Jahn–Teller effect (circles) and tungsten bronzes A_xWO_3 (A = Li, Na) stabilized by electronic effects (squares). A similar difference between the

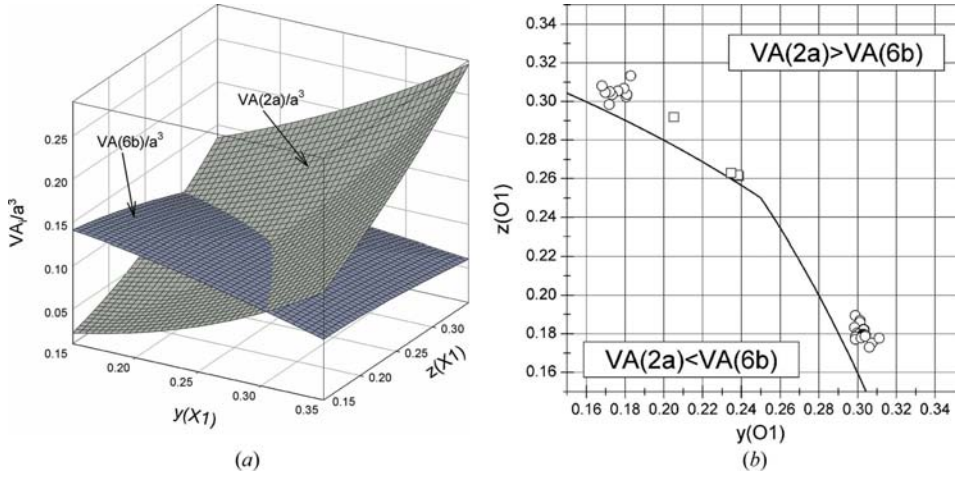

Figure 4
Volumes of A-site polyhedra for ($2a$) and ($6b$) Wyckoff positions normalized to the unit cell (a) and their ratio $VA(2a)/VA(6b)$ (b) as a function of $y(X1)$ and $z(X1)$ coordinates for the $Im3$ space group. Points represent experimental data from the ICSD. The $VA(2a) = VA(6b)$ curve (solid line in the bottom graph) is calculated by $z(X1) = \left\{2y(X1) + \left[-64y(X1)^3 - 12y(X1)^2 + 8y(X1) + 2\right]^{1/2}\right\}/\{4[4y(X1) + 1]\}$ for $y(X1) < z(X1)$ and $z(X1) = \left\{-8y(X1)^2 + 2y(X1) + \left[64y(X1)^4 - 32y(X1)^3 - 12y(X1)^2 + 2\right]^{1/2}\right\}/4$ for $y(X1) > z(X1)$.

functional dependence of inequivalent polyhedral volumes VA_i on atomic coordinates is observed for other space groups with multiple A sites and the higher number of inequivalent A sites, the more unlikely the perovskite structure will adopt that space group. This is consistent with the fact that ABX_3 perovskites with the space group *Immm* having four inequivalent A sites were not observed.

We notice that the preference of perovskites to adopt space groups having a single A and B site over those with multiple A and/or B sites is just a special case of the 5th Pauling's rule, also known as The Rule of Parsimony, according to which 'the number of essentially different kinds of constituents in a crystal tends to be small' (Pauling, 1929). Appealing to something like Pauling's rules may sound naive, but in fact the *ab initio* studies of $CaSiO_3$ perovskite energetics in the pressure range 0–150 GPa resulted in the conclusion that space groups with multiple A sites ($P4_2/nmc$, $I4/mmm$, $Im3$) are less stable than counterparts with single A and B sites such as *Pnma* or $I4/mcm$ (Caracas *et al.*, 2005; Jung & Oganov, 2005).

Finally, we would like to emphasize the obvious: it is the structural instabilities that drive changes in symmetry, not *vice versa*. Intuitive expectations that the symmetry should change gradually from the highest cubic to the lowest triclinic may result in the misinterpretation of phase diagrams. This was the case for the $PbZrO_3$–$PbTiO_3$ system in which the monoclinic phase, intermediate to the tetragonal and rhombohedral phases, was overlooked for decades (Noheda *et al.*, 1999). Another example is the recent report on the electron diffraction study of the notorious $Ca_xSr_{1-x}TiO_3$ system, where the sequence of phase transitions as a function of compositions is proposed to be $Pm3m \rightarrow I4/mcm \rightarrow C2/m \rightarrow P2_1/m \rightarrow Pnma$ (Woodward *et al.*, 2006). The statistics of polyhedral volume ratios presented in Fig. 3 suggests that this is not an impossible scenario.

4. Conclusions

The simple way of quantifying the degree of perovskite structure distortion with polyhedral volume ratios we have presented here allows streamlining the analysis of large amounts of published or new experimental data as it can be employed with software as simple as a spreadsheet (http://www.abx3.org, 2006). The analysis of PVR distribution for ABX_3 perovskites using crystallographic data accumulated in the Inorganic Crystal Structure Database has revealed the fields of stability of the most common space groups that can be useful for optimization parametric studies of perovskites. The lower limit of stability of the perovskite structure before it transforms to a post-perovskite $CaIrO_3$-type modification is estimated to correspond to $V_A/V_B \simeq 3.8$.

We thank reviewers for useful comments and suggestions and Dr A. Studer for enlightening discussions.

References

Aleksandrov, K. S. (1976). *Ferroelectrics*, **14**, 801–805.
Andrault, D. & Poirier, J. P. (1991). *Phys. Chem. Miner.* **18**, 91–105.
Balic Zunic, T. & Vickovic, I. (1996). *J. Appl. Chem.* **29**, 305–306.
Barnighausen, H. (1975). *Acta Cryst.* A**31**, S3.
Belsky, A., Hellenbrandt, M., Karen, V. L. & Luksch, P. (2002). *Acta Cryst.* B**58**, 364–369.
Brown, I. D. & Altermatt, D. (1985). *Acta Cryst.* B**41**, 244–247.
Caracas, R., Wentzcovitch, R., Price, G. D. & Brodholt, J. (2005). *Geophys. Res. Lett.* **32**, L06306.
Cotton, F. A. (1990). *Chemical Applications of Group Theory*, 3rd ed. New York: Wiley.
Fu, W. T. & Ijdo, D. J. W. (2006). *J. Solid State Chem.* **179**, 2732–2738.
Glazer, A. M. (1972). *Acta Cryst.* B**28**, 3384–3392.
Glazer, A. M. (1975). *Acta Cryst.* A**31**, 756–762.
Goldschmidt, V. M. (1926). *Naturwissenschaften*, **14**, 477–485.
Howard, C. J. & Stokes, H. T. (1998). *Acta Cryst.* B**54**, 782–789.
Howard, C. J. & Stokes, H. T. (2002). *Acta Cryst.* B**58**, 565.
ISI (2006). Web of Science. http://isiknowledge.com.
Jung, D. Y. & Oganov, A. R. (2005). *Phys. Chem. Miner.* **32**, 146–153.
Lufaso, M. W. & Woodward, P. M. (2001). *Acta Cryst.* B**57**, 725–738.
Magyari-Köpe, B., Vitos, L., Johansson, B. & Kollar, J. (2001). *Acta Cryst.* B**57**, 491–496.
Magyari-Köpe, B., Vitos, L., Johansson, B. & Kollar, J. (2002*a*). *Comput. Mater. Sci.* **25**, 615–621.
Magyari-Köpe, B., Vitos, L., Johansson, B. & Kollar, J. (2002*b*). *Phys. Rev. B*, **66**, 0192103.
Megaw, H. D. (1973). *Crystal Structures: A Working Approach.* Philadelphia: Saunders.
Michel, C., Moreau, J. M. & James, W. J. (1971). *Acta Cryst.* B**27**, 501.
Mitchell, R. H. (2002). *Perovskites: Modern and Ancient.* Thunder Bay, Ontario: Almaz Press.
Murakami, M., Hirose, K. Kawamura, K., Sata, N. & Ohishi, Y. (2004). *Science*, **304**, 855–858.
Noheda, B., Cox, D. E., Shirane, G., Gonzalo, J. A., Cross, L. E. & Park, S. E. (1999). *Appl. Phys. Lett.* **74**, 2059–2061.
Pauling, L. (1929). *J. Am Chem. Soc.* **51**, 1010–1026.
Poltavets, V., Vidyasagar, K. & Jansen, M. (2004). *J. Solid State Chem.* **177**, 1285–1291.
Thomas, N. W. (1996). *Acta Cryst.* B**52**, 954–960.
Thomas, N. W. (1998). *Acta Cryst.* B**54**, 585–599.
Thomas, N. W. & Beitollahi, A. (1994). *Acta Cryst.* B**50**, 549–560.
Woodward, D. I., Wise, P. L., Lee, W. E. & Reaney, I. M. (2006). *J. Phys. Condens. Matter*, **18**, 2401–2408.
Woodward, P. M. (1997). *Acta Cryst.* B**53**, 32–43.
Zhao, J., Ross, N. L. & Ange, R. J. (2004). *J. Phys. Condens. Matter*, **16**, 8763–8773.